Dyes and Pigments 95 (2012) 563–571

Contents lists available at SciVerse ScienceDirect

Dyes and Pigments

journal homepage: www.elsevier.com/locate/dyepig

A new class of solvatochromic material: Geometrically unsaturated Ni (II) complexes

P. Mosae Selvakumar[a], S. Nadella[a], R. Fröhlich[b], M. Albrecht[c], P.S. Subramanian[a,*]

[a] *Analytical Science Division, Central Salt and Marine Chemicals Research Institute, G.B.Marg, Bhavnagar, Gujarat, India*
[b] *Organisch-Chemisches Institut, Universitat Munster, Corrensstrasse 40, D-48149 Munster, Germany*
[c] *Institut fur Organische Chemie der RWTH – Aachen, 52074 Aachen, Germany*

ARTICLE INFO

Article history:
Received 3 December 2011
Accepted 11 May 2012
Available online 18 May 2012

Keywords:
Pyridine ligands
Nickel(II)
Binuclear complexes
Double stranded helicates
Solvent coordination
Solvatochromism

ABSTRACT

A series of Ni(II) double stranded binuclear complexes were synthesized upon treating the Ni(II) salts with series of diamino-bis-pyridine ligands, L_1H_2–L_4H_2 in 1:1 stiochiometric ratio. The Ni(II) centers existing in octahedral geometry, four of the coordination sites are occupied by two ligand strands, while the remaining two sites are occupied by solvent molecules in each metal centers. The Ni(II) complexes **1a**–**4a** and **1b**–**4b** are binuclear in nature with ClO_4 and PF_6 counter ions. The crystal structure obtained for complex **1b** ascertains the solvent coordination. Solvatochromism though a well established phenomena, such observation is reported first time in the present manuscript in the area of helicate chemistry. Thus the manuscript elicits the solvatochromic property of geometrically unsaturated helicates, by appropriately tuning the d-d transition, adapting suitable solvents.

1. Introduction

Ever since the terminology "helicate" was coined by Lehn [1–3] in 1987, varieties of single, double, triple and multistranded helical architectures with various metal ions were described [4–10]. All these complexes were mainly investigated due to their interesting structural features. Only in few cases examples were described [8–22], which possess a high potential for application. Classification of the helicates can either be done according to the number of strands or they can be classified as coordinatively saturated or unsaturated helicates [21,22]. The metal ion in the unsaturated helicates possesses labile/vacant sites. In the saturated systems, the metal ions are usually shielded and no chemical reactivity can generally be observed at the metal. Here the physical properties of the metal centers (luminescence [23,24], magnetism [25,26]) are of special interest. In the unsaturated case the metal ions can be approached by substrates and special reactivity or properties can be expected. Further, in the design of complex superstructures, with augmented number of helical strands, the importance of the unsaturated helicates was more or less ignored. Hence on comparison with the number of saturated helicates, the geometrically unsaturated helicates are rare in the literature. While the up-to-date studies on the helicates gave an understanding on the architectural aspects, the present decade is believed to bring out varieties of potential materials.

Colour being fascinating area of research [27–30], chromic behaviour of diverse organic and inorganic compounds gained immense research interest in view of the dye and pigments. In this context complexes of Ni(II) [31–36], Cu(II) [37–40] and Co(II) [41] are well known for their solvatochromic behaviour. Surprisingly so far no helicates were reported which possess solvatochromic behaviour. This opens up a broad field of application which can be envisaged for coordinatively unsaturated helicates. Their advantage is that they are usually more stable than corresponding mononuclear compounds. In addition, cooperative or additive effects may also be expected, if two unsaturated or labile metal units are fixed with a close distance to each other. The vacant sites can be filled up by suitable ligands, substrates or solvents. By doing this, it should be possible to tune the electronic properties of the metal ions towards achieving molecular recognition properties [42–48], DNA binding [49,50], appropriate catalysts [51] and chromic property etc. Having this in mind, the present manuscript describes the synthesis of a series of coordinatively unsaturated Ni (II) double stranded binuclear helicates. In this endeavor this present manuscript demonstrates that this class of compounds represents highly efficient solvatochromic material which produce different colors upon changing into different solvents.

---

* Corresponding author. Tel.: +91 278 2566970x673; fax: 91 278 2567760.
E-mail address: siva140@yahoo.co.in (P.S. Subramanian).

0143-7208/$ – see front matter © 2012 Elsevier Ltd. All rights reserved.
doi:10.1016/j.dyepig.2012.05.008

2. Experimental

2.1. Materials

All chemicals were purchased from sigma–aldrich & Co and were used as received. All the other reagents and solvents are commercially available and used without any further purification.

Microanalysis of the complexes was done using a Perkin–Elmer PE 2400 series II CHNS/O elemental analyzer. Electronic spectra were recorded on a HP diode array (model 8452A) UV-visible spectrophotometer. FT-IR spectra for KBr pellets (1% w/w) were recorded on a Shimadzu FT-COM 1 spectrophotometer. ^1H NMR spectra were recorded on a Bruker 200 MHz and 500 MHz spectrometer. TMS was used as internal reference, where non-aqueous solvents were employed.

2.2. Synthesis

2.2.1. Synthesis of ligands

***N,N′*-(1,4-phenylenebis (methylene) bis (1-(pyridine-2-yl) methanamine) (L_1)**: 2:1 methanolic solution of pyridine-2-carboxaldehyde (0.406 ml, 0.002 mol), and *p*-xylenediamine (0.318 g, 0.001 mol) were mixed and allowed for constant stirring with gentle heating for 2 h. The characteristic yellow solution for Schiff base was obtained by condensation. To this yellow color solution, $NaBH_4$ was added in excess and the reaction was allowed to run overnight. The color change of the ligand solution from yellow to colorless indicates the reduction of Schiff base. The resultant solution was evaporated and extracted using water/chloroform solvent mixture. Chloroform layer was collected and evaporated to dryness to get the compound. Yield: 95%. Anal. Data: calcd (found)% for $C_{20}H_{22}N_4$, C, 75.44 (75.32); H, 6.96 (6.84); N, 17.60 (17.51). ^1H NMR (δ, $CDCl_3$): 8.54–8.53 (d, Ar–CH, 2H), 7.62–7.59 (m, Ar–CH, 2H), 7.37–7.11 (m, Ar, 8H), 3.89 (s, CH_2, 4H), 3.80 (s, CH_2, 4H), 2.57 (br, NH). IR (ν, cm^{-1}): 3327 (weak, NH), 1588 (s, br). ESI [MS]: *m/z* calcd (found) for $C_{20}H_{22}N_4$ $(M + H)^+$, 319.19 (319.57).

***N,N′*-(1,3-phenylenebis (methylene)) bis (1-(pyridin-2-yl) methanamine), (L_2)**: The above procedure was repeated using *m*-xylenediamine in-place of *p*-xylenediamine. Yield 95%. Anal. Data: calcd (found)% for $C_{20}H_{22}N_4$; C, 75.44 (75.35); H, 6.96 (6.79); N, 17.60 (17.54). ^1H NMR (δ, $CDCl_3$): 8.53–8.52 (d, Ar–CH, 2H), 7.61–7.56 (t, Ar–CH, 2H), 7.35–7.10 (m, Ar, 8H), 3.87 (s, CH_2, 4H), 3.81 (s, CH_2, 4H), 2.58 (br, NH). IR (ν, cm^{-1}): 3306 (weak, NH), 1592 (s, br). ESI [MS]: *m/z* calcd (found) for $C_{20}H_{22}N_4$ $(M + H)^+$, 319.19 (319.68).

4,4′-methylenebis (*N*-(pyridin-2-ylmethyl) aniline), (L_3): The above procedure for L_1 was repeated using 4,4′-methylenedianiline instead of *p*-xylenediamine. Product was separated as white powder. Yield 92%. Anal. Data: calcd (found)% for $C_{25}H_{24}N_4$; C, 78.92 (78.76); H, 6.36 (6.31); N, 14.73 (14.65). ^1H NMR (δ, DMSO-D_6): 8.51–8.50 (d, 2H), 8.32 (s, 2H), 7.71–7.68 (t, 2H), 7.34–7.33 (d, 2H), 7.22–7.20 (t, 2H), 6.86–6.84 (d, 4H, 13), 6.48–6.47 (d, 4H), 6.16–6.14 (t, 2H, NH), 4.32–4.31 (d, 4H, CH_2), 3.55 (s, 2H, CH_2); IR (ν, cm^{-1}): 3368 (weak, NH), 1517 (s, intense). ESI [MS]: *m/z* calcd (found) for $C_{25}H_{24}N_4$ $(M + H)^+$, 381.48 (381.12).

4,4′-methylenebis (*N*-(quinolin-2-ylmethyl) aniline, (L_4): Following the above synthetic procedure for L_3 quinoline-2-carboxaldehye (0.314 g, 0.002 mol) was used in place of pyridine-2-carboxaldehyde. The product was separated as pale yellow powder. Yield 85%. Anal. Data: calcd (found) (%) for $C_{33}H_{28}N_4.H_2O$; C, 79.49 (80.10); H, 6.06 (5.92); N, 11.24 (10.58). ^1H NMR Data (δ, CD_2Cl_2): 8.17–7.43 (m, Ar–CH, 12H), 7.04–7.00 (d, Ar–CH, 4H), 6.70–6.66 (d, Ar, 4H), 5.16 (br, NH), 4.60–4.58 (d, CH_2, 4H), 3.76 (s, CH_2, 2H). IR (ν, cm^{-1}): 3317 (weak, NH), 1521 (s, intense). ESI [MS]: *m/z* calcd (found) for $C_{33}H_{28}N_4$ $(M + H)^+$ 481.24 (481.43).

2.2.2. Synthesis of double helicate complexes

2.2.2.1. General procedures for the synthesis of complexes. All complexes **1a**, **2a**, **3a** and **4a** were synthesized using 1:1 $Ni(ClO_4)_2.6H_2O$ and appropriate ligands. Similarly the corresponding PF_6 complexes **1b**, **2b**, **3b** and **4b** were obtained following anion metathesis using NH_4PF_6.

$[Ni_2(L_1)_2(CH_3CN)_4]$ $(ClO_4)_4$, (1a): The ligand L_1 (0.318 g, 0.001 mol) dissolved in acetonitrile was mixed with methanolic solution of $[Ni(ClO_4)_2].6H_2O$ (0.365 g, 0.001 mol) and allowed for continuous stirring and the resultant light blue precipitate appeared. The precipitate obtained was separated and dried. Yield: 85%. Anal. Data: calcd (found)% for $C_{48}H_{56}Cl_4N_{12}Ni_2O_{16}$ C, 43.80 (43.69); H, 4.29 (4.21); N, 12.77 (12.64). UV-Vis [CH_3CN, λ/nm, $(\varepsilon/M^{-1}cm^{-1})$], 436 $(15)^{sh}$, 560 (21), 786^{sh} (11), 921 (20). IR (ν, cm^{-1}): 3411(br, NH), 1094 (s, intense), 625 (st, intense). ESI [MS]: *m/z* calcd (found) for $C_{40}H_{44}Ni_2Cl_3N_8O_{12}$ $(M{-}ClO_4)^+$; 1051.08 (1051.71).

$[Ni_2(L_1)_2(CH_3CN)_4]$ $(PF_6)_4$, (1b): The above synthesized complex **(1a)** dissolved in acetonitrile and mixed with methanolic solution which contains excess amount of ammonium hexaflouro phosphate and heated to 60 °C with continuous stirring for 1 h provided pale blue precipitate. The precipitate obtained was separated and dried. Yield: 95%. Anal. Data: calcd (found)% for $C_{48}H_{56}F_{24}N_{12}Ni_2P_4$, C, 38.48 (38.41); H, 3.77 (3.72); N, 11.22 (11.18). UV-Vis [CH_3CN, λ/nm, $(\varepsilon/M^{-1}cm^{-1})$]: 567 (40), 796^{sh}(20), 925 (26). IR (ν, cm^{-1}): 3331(br, NH), 1571 (st, intense), 841 (s, intense). ESI [MS]: *m/z* calcd (found) for $C_{40}H_{44}Ni_2F_6N_8P$ $(M\text{-}3PF_6{+}H)^{4+}$, 898.21 (898.97).

$[Ni_2(L_2)_2(CH_3CN)_4]$ $(ClO_4)_4$, (2a). The ligand L_2 (0.318 g, 0.001 mol) dissolved in acetonitrile was mixed with methanolic solution of $[Ni(ClO_4)_2].6H_2O$ (0.370 g, 0.001 mol) and allowed to continuous stirring for 3 h provided pale blue precipitate. The precipitate obtained was separated and dried. Yield: 90%. Anal. Data: calcd (found)% for $C_{48}H_{56}Cl_4N_{12}Ni_2O_{16}$, C, 43.80 (43.75); H, 4.29 (4.24); N, 12.77 (12.59). UV-Vis [CH_3CN, λ/nm, $(\varepsilon/M^{-1}cm^{-1})$]: 435.06 $(57)^{sh}$, 541 (40), 780^{sh} (20), 887 (24). IR (ν, cm^{-1}): 3433 (br, NH), 1092 (s, intense) 0.618 (s, intesne), ESI [MS]: *m/z* calcd (found) for $C_{40}H_{44}Cl_3Ni_2N_8O_{12}$ $(M - ClO_4)^+$; 1051.08 (1051.32).

$[Ni_2(L_2)_2(CH_3CN)_4]$ $(PF_6)_4$, (2b): The above synthesized complex **(2a)** was dissolved in acetonitrile and treated with methanolic solution of excess ammonium hexaflouro phosphate and heated to 60 °C with continuous stirring for 1 h provided pale blue precipitate. The precipitate obtained was separated and dried. Yield: 94%. Anal. Data: calcd (found)% for $C_{48}H_{56}F_{24}N_{12}Ni_2P_4$, C, 38.48 (38.37); H, 3.77 (3.68); N, 11.22 (11.31). UV-Vis [CH_3CN, λ/nm, $(\varepsilon/M^{-1}cm^{-1})$]: 441$(83)^{sh}$, 532 (57), 774^{sh} (33), 883 (37). IR (ν, cm^{-1}): 3407 (br, NH), 1545 (st, intense), 844 (s, intense). MS ESI [MS]: *m/z* calcd (found) for $C_{40}H_{44}Ni_2F_6N_8P$ $(M\text{-}3PF_6)^{3+}$; 898.20 (898.97).

$[Ni_2(L_3)_2(CH_3CN)_4]$ $(ClO_4)_4$, (3a): The ligand L_3 (0.380 g, 0.001 mol) dissolved in acetonitrile was mixed with methanolic solution of $[Ni(ClO_4)_2].6H_2O$ (0.365 g, 0.001 mol) and allowed to continuous stirring for 3 h provided pale blue precipitate. The precipitate obtained was separated and dried. Yield: 80%. Anal. Data: calcd (found)% for $C_{58}H_{60}Cl_4N_{12}Ni_2O_{16}$, C, 48.36 (48.32); H, 4.20 (4.17); N, 11.67 (11.61). UV-Vis [DMF, λ/nm, $(\varepsilon/M^{-1}cm^{-1})$]: 500 (1047), 770 (11), 956.57 (20). IR (ν, cm^{-1}): 3360 (br, NH), 1100 (s, intesne), 625 (s, intesne). ESI [MS]: *m/z* calcd (found) for $C_{50}H_{48}Cl_3N_8Ni_2O_{12}$ $(M{-}ClO_4)^+$; 1175.11 (1174.87); $[(M - ClO_4){+}H]^{2+}$ 1176.12 (1176.86).

$[Ni_2\,(L_3)_2\,(CH_3CN)_4]\,(PF_6)_4$ (3b): The above synthesized complex **(3a)** dissolved in acetonitrile and mixed with methanolic solution which contains excess amount of ammonium hexaflouro phosphate and heated to 60 °C with continuous stirring for 1 h provided pale blue precipitate. The precipitate obtained was separated and dried. Yield: 60%. Anal. Data: calcd (found)(%) for $Ni_2C_{50}H_{48}F_{24}N_8P_4.4H_2O$: C, 39.24 (39.02); H, 3.69 (2.97); N, 7.32 (6.83). IR Data (ν, cm^{-1}): 3322 (br, NH), 1543 (st, intense), 845 (s, intense).UV-Vis [DMF, λ/nm, (ε/$M^{-1}cm^{-1}$)]:526.38 (132), 979.65 (35). ESI [MS]: *m/z* calcd (found) for $Ni_2C_{50}H_{48}F_{12}N_8P_2Na$, $(M\text{-}2PF_6\text{+}Na)^{3+}$: 1189.19 (1189.05).

$[Ni_2(L_4)_2(H_2O)_2]$ $(ClO_4)_4$ (4a): The ligand L_4 (0.481 g, 0.001 mol) dissolved in dichloromethane was mixed with methanolic solution of Ni $(ClO_4)_2.6H_2O$ (0.366 g, 0.001 mol) and allowed for continuous stirring 2 h and warmed at 60 °C for 1 h. The color change from yellow to wine red indicates the complexation. The solution is evaporated to give reddish brown solid. Yield: 90%. Anal. Data: calcd (found)(%) for $Ni_2C_{66}H_{56}Cl_4N_8O_{16}.2H_2O$: C, 52.41 (52.54); H, 4.00 (3.27); N, 7.41 (6.83). IR Data (ν, cm^{-1}): 3415 (br, NH), 1098 (s, intense), 625 (s, intense). UV-Vis [CH_3CN, λ/nm, (ε/$M^{-1}cm^{-1}$)]: 550.23 (409), 763.36 (3.8), 951.64 (23.7). ESI [MS]: *m/z* calcd (found) for $Ni_2C_{66}H_{56}Cl_3N_8O_{12}$ $(M{-}ClO_4\text{+}H)^{2+}$: 1378.18 (1378.32).

$[Ni_2(L_4)_2(H_2O)_2]$ $(PF_6)_4$ (4b): The above synthesized complex **(4a)** mixed with excess amount of ammonium hexaflouro phosphate in methanol solution and heated to 60 °C with continuous stirring for 1 h provided red coloured precipitate. The precipitate obtained was separated, washed with cold methanol and dried. Yield: 60%. Anal Data: calcd (found) (%) for $Ni_2C_{66}H_{56}F_{24}N_8P_4.2H_2O$: C, 46.78 (46.33); H, 3.57 (3.49); N, 6.61 (6.32). IR Data (ν, cm^{-1}): 3329 (br, NH), 1513 (st, intense), 835 (s, intense). UV-Vis [CH_3CN, λ/nm, (ε/$M^{-1}cm^{-1}$)]: 488.84 (495), 1058.57 (14.2). ESI [MS]: *m/z* calcd (found) for $Ni_2C_{66}H_{56}F_6N_8P$, $(M\text{-}3PF_6\text{+}H)^{4+}$: 1222.31 (1222.58).

CAUTION! Perchlorate salts of metal complexes are potentially explosive and should be handled with great care.

2.3. X-ray crystallography

Data set was collected with a Nonius Kappa CCD diffractometer, equipped with a rotating anode generator. Programs used: data collection COLLECT [52], data reduction Denzo-SMN [53], absorption correction Denzo [54], structure solution SHELXS-97 [55], structure refinement SHELXL-97 [56], graphics SCHAKAL [57]

CCDC 798728 contains the supplementary crystallographic data for **1b**. These data can be obtained free of charge at www.ccdc.cam.ac.uk/conts/retrieving.html [or from the Cambridge Crystallographic Data Centre, 12 Union Road, Cambridge CB2 1EZ, UK; fax: (internet.) +44 (1223) 336-033, E-mail: deposit@ccdc.cam.ac.uk.

3. Results and discussion

The bis-pyridine ligands L_1, L_2, L_3 and L_4 were synthesized [58] and characterized starting from their imine precursors following the standard $NaBH_4$ reduction. The completion of the reduction process was monitored using ^1H NMR and the respective CH_2 and NH peaks were found appeared, while the corresponding CH=N peak were disappeared. All these ligands possess two amine and two pyridyl nitrogens, while the two aminomethyl pyridins are separated by aromatic spacers as shown in Scheme 1. The attempt to synthesize triple, double and single stranded helicates with appropriate 3:2, 2:2 and 1:1 ligand:Ni(II) ratio mainly resulted in double stranded helicates. Only in few cases triple stranded helicates were obtained. However the present study primarily explores the coordinatively unsaturated complexes, here we report only the coordinatively unsaturated double stranded helicates. The tetracationic complexes **1a**–**4a** & **1b**–**4b** were obtained from the corresponding ligands L_1, L_2, L_3 and L_4 respectively, with 1:1 Ni(II): ligand ratio. While the perchlorate complexes **1a**–**4a** were synthesized using $Ni(ClO_4)_2.6H_2O$, the respective hexafluorophospate complexes of **1b**–**4b** were obtained from **1a**–**4a** by anion metathesis approach by using ammoniumhexafluorophosphate. The MS spectra obtained for complex **1a**–**4a** and **1b**–**4b** indicate the formation of the respective complexes (S2). Finally, numerous attempts to obtain suitable single crystals lead to the crystal structure of **1b** $[Ni(L_1)(CH_3CN)_2]_2(PF_6)_4$. The IR spectra recorded for all the perchlorate and hexafluorophosphate complexes confirms their presence in ionic form. The hexa flurophosphate complexes giving single peak at around 840 cm^{-1} which not only ruled out any significant interaction with Ni(II) metal center, but also confirms their existence in the ionic form [59–61]. Similar to the hexafluorophosphate anion, the perchlorate counter ion in complex **1a**–**2a** giving characteristic IR bands, respect to their *Td* modes at around 1100 and 625 cm^{-1} and indicates their existence in ionic form [62,63]

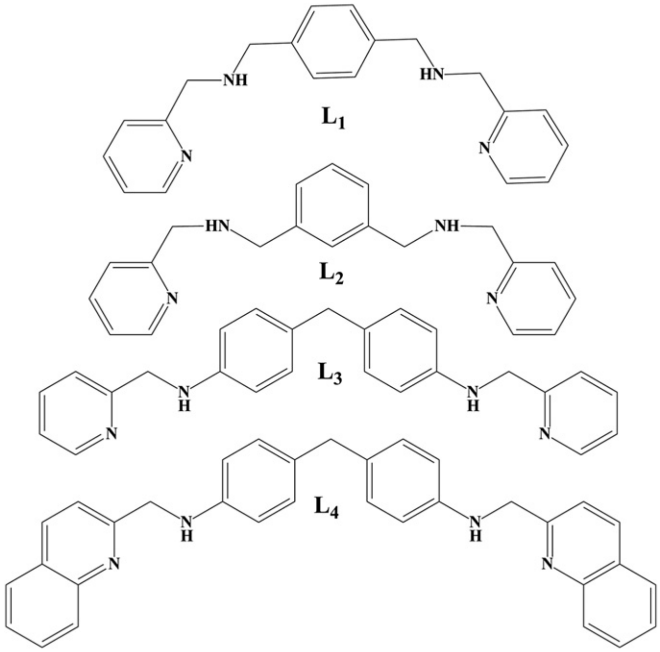

Scheme 1. Various ligand systems used in the helical construction.

3.1. Crystal structures of complex *1b*

The crystal structure of **1b** with atom numbering scheme is depicted in Fig. 1 (i). The molecular structure in the crystal [64] exhibits C2 symmetry. Fig. 1 shows the dinuclear Ni(II) centers are wrapped by two ligand strands L_1. The Ni(II) centers are separated by 9.00 Å. They adopt a distorted octahedral geometry with four PF_6 counter ions residing outside the coordination sphere of the metal. While the amino nitrogen (NH17; Ni(1)–NH (17) = 2.140 Å) of one ligand strand and nitrogen from one acetonitrile (N41; Ni(1)–N (41) = 2.101 Å) are occupying the axial sites of Ni (1), the equatorial sites are occupied by two pyridyl nitrogens of the two different strands (N (24) & N (10); Ni(1)–N (24) = 2.008; Ni(1)–N (10) = 2.090 Å) and the other two by amino nitrogen (N8H; Ni(1)–N (8) = 2.127 Å) and acetonitrile nitrogen (N (31); Ni(1)–N (31) = 2.084 Å). Both the ligand strands in their neutral form possess two amine and two pyridyl nitrogens

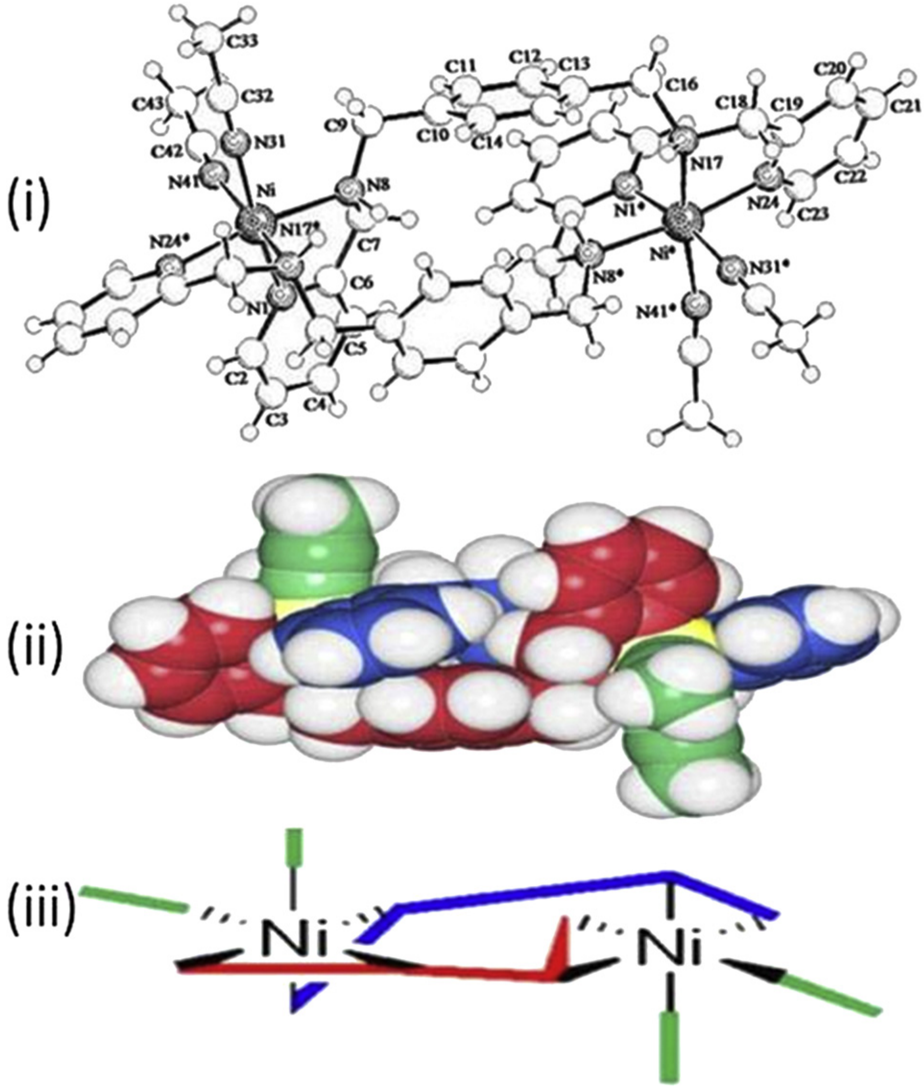

Fig. 1. (i) Structure of tetracationic complex **1b** with atom numbering scheme (ii) Space filling model (iii) Stick representation.

and binds the Ni(II) metal centers. Two *cis*-arranged acetonitrile molecules filling up each coordination site, resulted in the distorted octahedral geometry. The two ligands in the dinuclear coordination compound **1b** are binding in different fashion, is shown in blue and red (Fig. 1 (ii) and iii). This figure illustrates that one ligand (blue) is coordinating one nickel ion from the "side" while the other is located in the internal void "in-between" the two metals. The second ligand (red) is arranged with a curved shape in order to chelate one of the two nickel atoms. The coordination sites which are occupied by the solvent molecules (green) are oriented in opposite direction and thus are preventing the formation of the corresponding triple stranded helicate in this case. As seen in Fig. 1 (i), four of the six sites in the Ni(II) octahedral sphere are occupied by the pyridyl and amino nitrogen of the ligand strands, while the remaining two sites at each Ni(II) center are occupied by solvent molecules. These solvents are labile and can easily be replaced by various other solvents or substrates depending upon the demand. The possibility of functionalization of this labile site though seems multidirectional, the aim of the present study limits to explore the solvatochromic property using different solvents depending on their increasing donor strength.

3.2. *Solvatochromism*

The complex (**1**–**3**) **a, b** in the solid state are generally light blue in color, while the complex **4a**, **4b** gives an entirely different color i.e. brownish red in the respective solid state. The complex **1a**, **2a** and **3a** possessing ClO_4 counter ions, they are found to be pale blue in color, while the respective counterparts with PF_6 anions **1b**, **2b** and **3b** are depicting little intense blue. Though both of them looking almost similar in color, the subtle change in their intensity may signify the role of counter ions. This may be due to the difference in the anions which may have some supramolecular contact, since they are not directly involved in the coordination. However the solvent effects being dominant which has direct effect on the d-d transition, the color changes on changing the solvent are quite visible. The complexes **4a** and **4b** though exists in brown color, the **4a** with ClO_4 gives dark brown, while the PF_6 counterpart gives light brown which may be attributed for the combined role played by the counter ion as well as quinoline fluorophore substituted on the ligand moiety. Interestingly, the complexes give different colors in different solvents. The observed color changes for **1**–**3** **a, b** are depicted in Fig. 2, while the complex **4a**, **4b** are presented in Fig. 3. The crystal structure obtained for complex **1b**

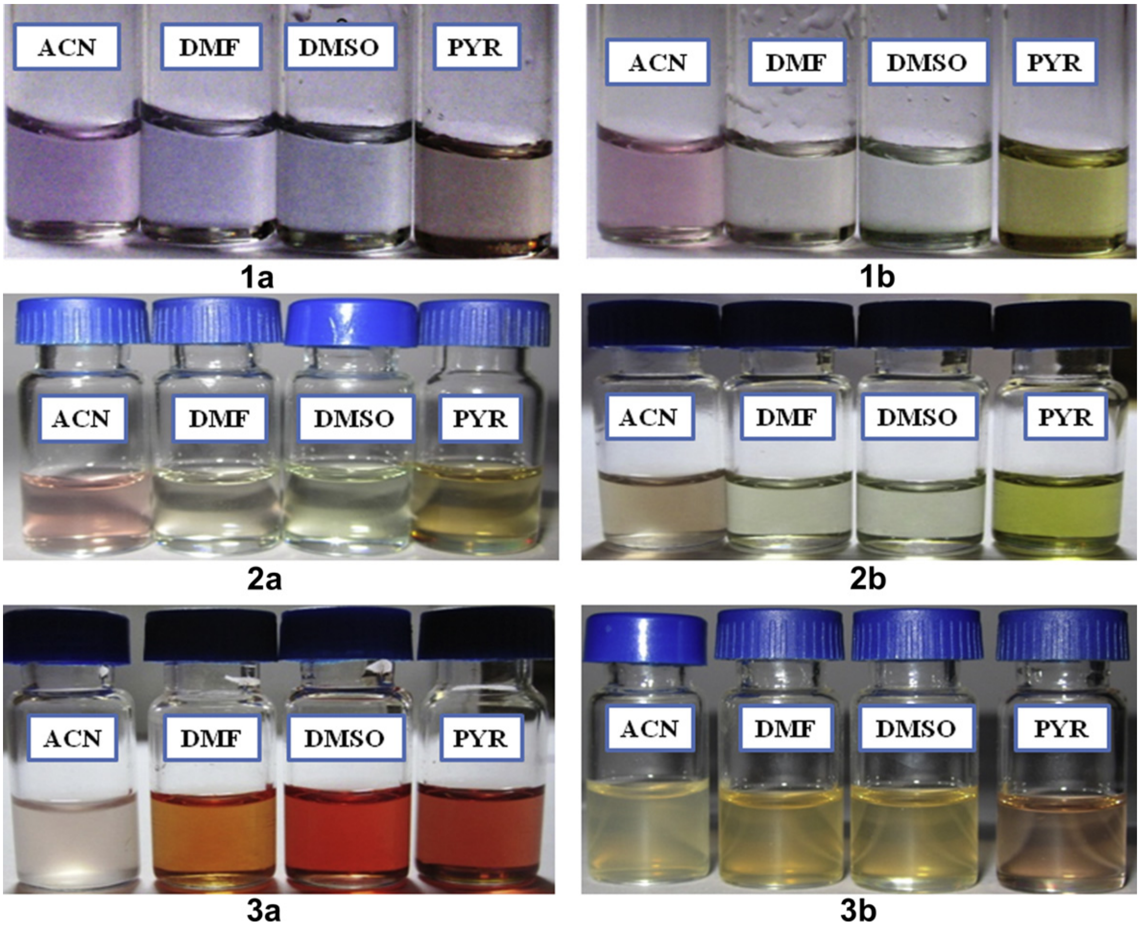

Fig. 2. Solvatochromism shown by complexes $[Ni_2 (L_1)_2 (S)_4]$,$(ClO_4)_4$ **1a**, $[Ni_2 (L_1)_2 (S)_4] (PF_6)_4$ **1b** and $[Ni_2 (L_2)_2 (S)_4](ClO_4)_4$ **2a**, $[Ni_2 (L_2)_2 (S)_4](PF_6)_4$ **2b** and $[Ni_2 (L_3)_2 (S)_4](ClO_4)_4$ **3a**, $[Ni_2 (L_3)_2 (S)_4](PF_6)_4$ **3b**, where “S” denote the solvents.

illustrates the coordination of four labile solvent molecules in each binuclear system. The aim was to replace them by appropriate solvents simply by dissolving them in the respective solvent. Complex **1a** leads to pink, violet, blue and wine red solutions, while complex **1b** with hexafluorophosphate results in wine red, pale yellow, pale blue and green colors (Fig. 2). A similar approach to complex **2a**, **2b** and **3a**, **3b** also depict a subtle color change (Fig. 2). While the complex **1** and **2** behaving almost similar with subtle difference in their color change, the complex **4a** and **4b** gives wide range of solubility with wide range of colors from violet in pyridine to wine red in tetrahydrofuran (Fig. 3). Such solvatochromic behaviour was already known in coordination chemistry. However, the present study is the first in the area of helicate chemistry and reveals that unsaturated helicates represent a most favorable platform for such studies. Although a significant number of unsaturated double stranded binuclear helicates is reported in the literature, so far no report has been found on the solvatochromic behaviour.

Surprisingly, the elemental data though showed existence of solvents, the MS spectra did not give any evidence for the existence of solvent molecules. This may be attributed for the highly labile coordination nature of the solvents. In the newly reported binuclear Ni(II) complexes, the d-d transition on the Ni(II) metal centre with its d^8 configuration required an in-depth analysis by electronic spectroscopy (UV-Vis NIR) as discussed below.

All the Ni(II) complexes are soluble in a variety of coordinating solvents, the corresponding changes in the UV-Vis spectrum with respect to different solvents were studied. Figs. 2 and 3 illustrate the color of the complexes in different solvents, in which the respective electronic spectra for **1**–**3** & **4** were recorded. The electronic spectra of **4a** and **4b** were recorded in a wide range of solvents such as THF, EtOH, CH_3OH, CH_3CN, DMF, DMSO and Pyridine and the respective data are depicted in Table 1. The complexes **1a** and **1b** dissolved in acetonitrile, DMF and DMSO show three main bands in the range of 434–436 nm, 560–590 nm and 920–960 nm as shown in Fig. 4. An additional weak transition was observed in the range of 775–785 nm. Interestingly the spectra recorded in pyridine shows two weak transitions, one at 775–785 nm similar as observed for the other solvents, the second one was detected at 1150 nm. The peak in the range 560–590 nm, 920–960 nm and the shoulder at 775–785 nm were detected in almost all spectra, while the peak at 434–436 nm appeared as a shoulder only in acetonitrile and pyridine. In other solvents it probably is merged with ligand centered transitions and/or ligand to metal charge transfer bands, which appear between 200 and 435 nm.

All these peaks showing bathochromic shift (shift towards longer wavelength) with increasing Guttmann donor number [65] of the solvent. The change in the colors can be termed as positive solvatochromism. A similar spectral behaviour was observed for complex **2a** and **2b**, illustrating a negligible effect on the d-d transition, due to the subtle difference in ligand strength caused by *m*-xylene on L_2 over *p*-xylene on L_1. The band at 434–436 nm for complex **1a**, **1b** and **2b** dissolved in acetonitrile and pyridine were attributable to ν_1 in the range of 22675–22988 cm^{-1} and 22883–23041 cm^{-1} indicating the respective 10Dq on these complexes. The increase in the 10Dq suggests that the LFSE of

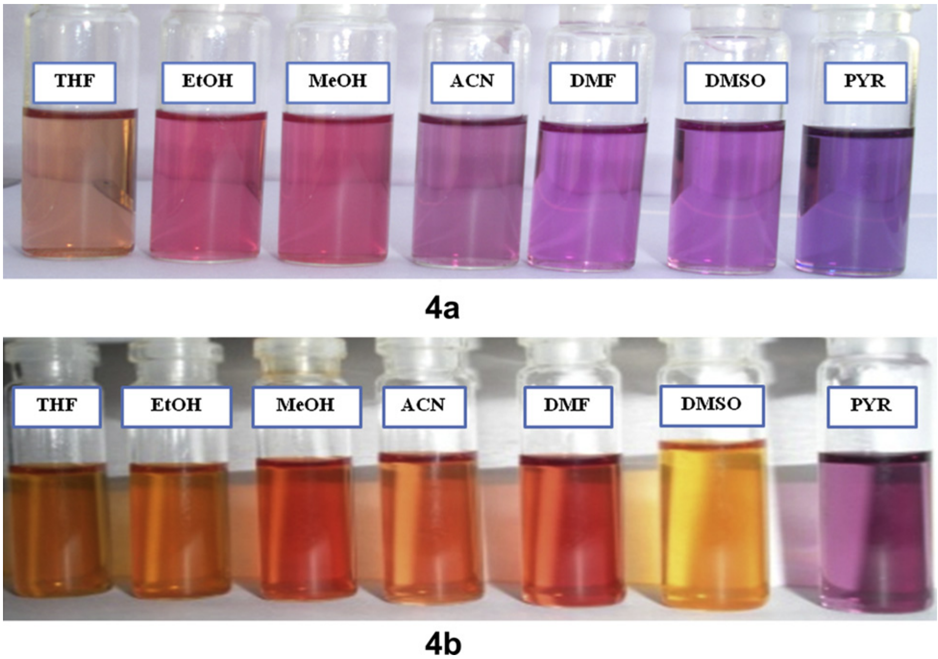

Fig. 3. Solvatochromism exhibited by $[Ni_2 (L_4)_2 (S)_4](ClO_4)_4$, **4a** and $[Ni_2 (L_4)_2 (S)_4] (PF_6)_4$ **4b**, where “S” denote the solvent.

Table 1
Table for UV-Vis spectral data for complexes.

Com	Solvent	Wavelength, nm (ε)
1a	CH_3CN	436.07 (15), 560.52 (21), 786.75 (11)^{Sh}, 921.14 (20)
	DMF	576.98 (17), 778.90 (10)^{Sh}, 931.90 (20)
	DMSO	587.52 (16), 785.18 (7)^{Sh}, 953.22 (21)
	PYR	434.48 (34), 578.86 (20), 778.00 (5)^{Sh}, 950.76 (14), 1142.42 (16).
1b	CH_3CN	567.12 (40), 796.40 (19)^{Sh}, 925.58 (26)
	DMF	574.49 (24), 785.73 (6)^{Sh}, 947.67 (16)
	DMSO	575.95 (27), 787.57 (10)^{Sh}, 947.27 (20)
	PYR	436.47 (22), 589.21 (25), 787.20 (5)^{Sh}, 961.28 (16), 1125.42 (16).
2a	CH_3CN	435.06 (57), 541.23 (40), 780.48 (20)^{Sh}, 887.67 (24),
	DMF	573.94 (17), 773.78 (6.5)^{Sh}, 932.95 (16.5)
	DMSO	581.45 (19), 781.41 (6.5)^{Sh}, 963.90 (20), 1164.23 (17.6).
	PYR	437.37 (72), 574.26 (25), 781.41 (5.5)^{Sh}, 953.97 (13), 1138.79 (18).
2b	CH_3CN	441.23 (83.5), 532.04 (57), 774.55 (33)^{Sh}, 883.99 (37)
	DMF	570.09 (21), 779.32 (10), 944.48 (17.5)
	DMSO	576.08 (19), 781.08 (9), 961.29 (18), 1165.09 (20).
	Pyr	437.50 (75), 580.15 (21), 782.58 (5)^{Sh}, 965.31 (11), 1140.26 (16).
3a	DMF	500.47 (1047), 770.4 (11), 956.57 (20).
	DMSO	512.12 (1742), 788.42 (14), 983.74 (19), 1161.33 (13).
	PYR	518.09 (770), 791.42 (9.7), 990.46 (14), 1169.29 (7.9).
4a	CH_3CN	550.23 (409), 763.36 (3.8), 951.64 (23.7)
	THF	489.82 (268)
	CH_3OH	524.94 (750), 761.91 (12), 975.910 (9), 1134.83 (9)
	DMF	541.81 (424), 936.11 (4), 1100.13 (12)
	DMSO	543.30 (199), 778.89 (14.7), 994.83 (5.7)
	PYR	567.02 (492), 807.28 (7.7), 963.05 (11)
4b	CH_3CN	488.84 (495), 1058.57 (14.2)
	THF	504.46 (649), 974.15 (35)
	CH_3OH	534.34 (545), 991.62 (16), 1166.49 (16)
	EtOH	494.41 (629), 987.58 (26)
	DMF	564.54 (351), 993.63 (5.6), 1141.42 (7.6)
	DMSO	535.74 (544), 977.48 (22.3), 1129.32 (19.3)
	PYR	509.35 (609), 1038.86 (17.1)

[^{sh}] shoulder.

pyridine is stronger than of acetonitrile. Unfortunately in complex **3a** and **3b**, it was not possible to locate the band corresponding to ν_1. It may have merged with the ligand centered transition, which might have appeared lower than 435 nm where the ligand centered bands are dominant. The high energy shift could be caused by the combined effect of ligand strength and the solvent strength on ν_1. The complexes **4a**, **4b** show an absorption in the range of 500–570 nm and an absorption in the range of 930–1040 nm, representing the band which corresponds to ν_2 and ν_3 respectively.

Free nickel(II) ions [66] in d^8 configuration possess Russel Saunders terms ^3F, ^3P, ^1D, ^1G, ^1S. The ground state ^3F of the octahedral geometry can split into $^3A_{2g}(F)$, $^3T_{2g}(F)$ and $^3T_{1g}(F)$. Similarly ^3P into $^3T_{1g}(P)$; ^1D into $^1E_{1g}(D)$ and $T_{2g}(D)$; ^1G into $^1A_{1g}(G)$, $^1T_{1g}(G)$, $^1T_{2g}(G)$ and $^1Eg(G)$; and ^1S into $^1A_{1g}(S)$ once a ligand field is introduced. Among this the transitions $^3A_{2g}(F) \rightarrow {}^3T_{2g}(F)$, $^3A_{2g}(F) \rightarrow {}^3T_{1g}(F)$ and $^3A_{2g}(F) \rightarrow {}^3T_{1g}(P)$ are generally termed spin allowed transitions. The two spin forbidden transitions are $^3A_{2g}(F) \rightarrow {}^1E_{1g}(D)$ and $^3A_{2g}(F) \rightarrow {}^1T_{2g}(D)$. Generally three intense spin allowed and two weak spin forbidden bands are expected for Ni (II), d^8 configuration in octahedral geometry [67,68]. Accordingly the complex **1a**, **1b**, **2a** and **2b** upon dissolving in acetonitrile and pyridine reveal three bands as stated above along with a shoulder at 770 nm. The three intense bands represent the three spin allowed d-d transitions from the ground state,$^3A_{2g}(F) \rightarrow {}^3T_{2g}(F) = 950$ nm; $^3A_{2g}(F) \rightarrow {}^3T_{1g}(F) = 550$ nm; $^3A_{2g}(F) \rightarrow {}^3T_{1g}(P) = 360$ nm. Weak features, due to the spin forbidden transitions $^3A_{2g}(F) \rightarrow {}^1E_{1g}(D)$ also occur, at energies between the $^3A_{2g}(F) \rightarrow {}^3T_{1g}(F)$ and $^3A_{2g}(F) \rightarrow {}^3T_{2g}(F)$ transitions, while a further week transition was observed at around 1150 nm representing $^3A_{2g}(F) \rightarrow {}^1T_{2g}(D)$ transition. The observation of this spin forbidden transition is thought to be facilitated by the close proximity of $^3A_{2g} \rightarrow {}^3T_{2g}$ and $^3A_{2g}(F) \rightarrow {}^1E_g$ transitions, which leads to a strong mixing through spin–orbit coupling.

Based on the above study, the Scheme 2 explains the observed solvatochromic behaviour of complex **1**, and gives the pictorial representation for all the other complexes reported in the manuscript.

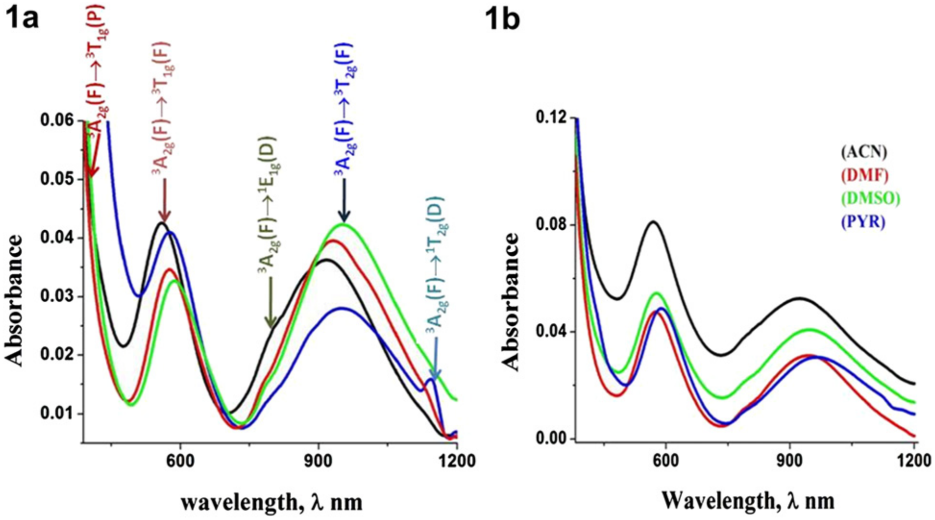

Fig. 4. UV-Vis spectra for complex **1a** and **1b** in different solvents.

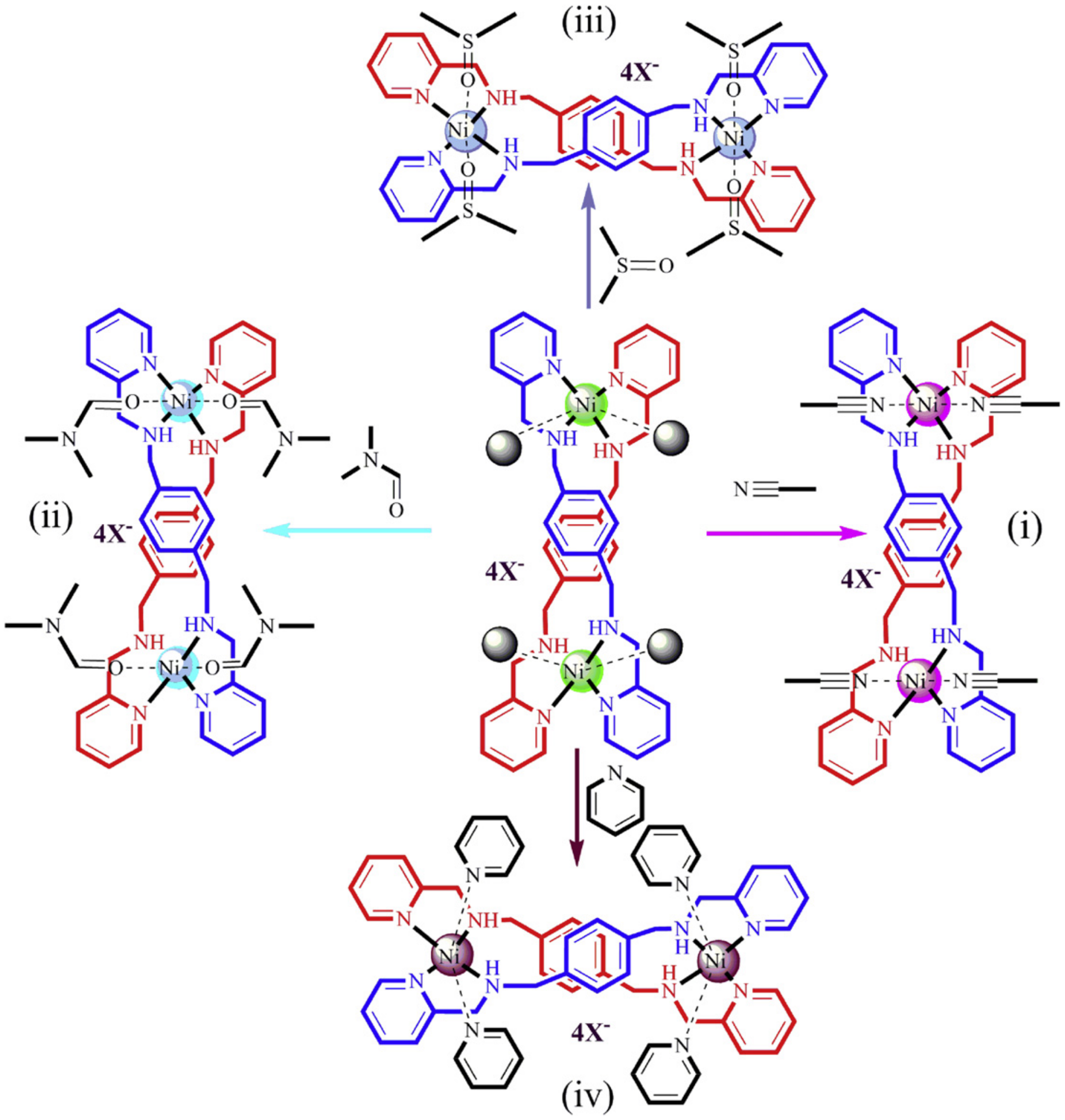

Scheme 2. Schematic diagram of solvent coordination fulfilling labile sites in Ni (II) helicates **1**. (i) CH_3CN. (ii) DMF. (iii) DMSO. (iv) Pyridine.

4. Conclusion

In summary, a series of coordinatively unsaturated Ni(II) double stranded helicates were synthesized and their solvatochromic properties were demonstrated for the first time. The described coordinatively unsaturated helicates possess labile solvent molecules, which can be substituted upon the change of the solvent and studied their electronic transitions using electronic spectra. Our further work in this direction is under progress to use those labile sites, which provides potential scope for a wide range of applications in the area of biological science as a marker.

Acknowledgements

The authors PS, PMSK and SN gratefully acknowledge the DST and CSIR New Delhi, India for their financial support.

Appendix A. Supplementary data

Supplementary data associated with this article can be found, in the online version, at doi:10.1016/j.dyepig.2012.05.008.

References

[1] Lehn JM. Supramolecular Chemistry, concepts and perspectives. Weinheim: VCH; 1995.

[2] Baxter PN. In: Atwood JL, Davies JED, MacNicol DD, Vögtle F, Lehn JM, editors. Comprehensive supramolecular chemistry, vol. 9. Oxford: Pergamon; 1996. p. 165.

[3] Swiegers GF, Malefetse TJ. New self-assembled structural motifs in coordination chemistry. Chem Rev 2000;100(9):3483–538.

[4] Albrecht M. Let's twist again" double-stranded, triple-stranded, and circular helicates. Chem Rev 2001;101(11):3457–98.

[5] Zelewsky AV. Stereoselective synthesis of coordination compounds. Coord Chem Rev 1999;190-192:811–25.

[6] Caulder DL, Raymond KN. Supermolecules by design. Acc Chem Res 1999; 32(11):975–82.

[7] Machado VG, Baxter PNW, Lehn JM. Self-Assembly in self-organized inorganic systems: a view of programmed metallosupramolecular architectures. J Braz Chem Soc 2001;12(4):431–62.

[8] Bünzli J-CG. Lanthanide luminescence for biomedical analyses and imaging. Chem Rev 2010;110(5):2729–55.

[9] Eliseeva SV, Bünzli J-CG. Lanthanide luminescence for functional materials and bio-sciences. Chem Soc Rev 2010;39(1):189–227.

[10] Piguet C, Bünzli J-CG, Gschneider Jr KA, Percharsky VK. Self assembled lanthanide helicates: from basic thermodynamics to applications [Chapter 247]. LCSL-Elsevier; 2009.

[11] Pascu GI, Holtz ACG, Sanchez-Cano C, Kariuki BM, Hannon MJ. Dinuclear ruthenium(II) triple-stranded helicates: luminescent supramolecular cylinders that bind and coil DNA and exhibit activity against cancer cell lines. Angew Chem Int Ed 2007;46(23):4374–8.

[12] Uerpmann C, Malina J, Pascu M, Clarskson GJ, Moreno V, Rodger A, et al. Design and DNA binding of an extended triple-stranded metallo-supramolecular cylinder. Chem Eur J 2005;11(6):1750–6.

[13] Telfer SG, Sato T, Kuroda R. Noncovalent ligand strands for transition-metal helicates: the straightforward and stereoselective self-assembly of dinuclear double-stranded helicates using hydrogen bonding. Angew Chem Int Ed 2004; 43(5):581–4.

[14] Telfer SG, Kuroda R. The versatile, efficient and stereoselective self-assembly of transition-metal helicates by using hydrogen-bonds. Chem Eur J 2005; 11(1):57–68.

[15] Telfer SG, Sato T, Kuroda R, Lefebvre J, Leznoff DB. Dinuclear complexes of chiral tetradentate pyridylimine ligands: diastereoselectivity, positive cooperativity, anion selectivity, ligand self-sorting based on chirality and magnetism. Inorg Chem 2004;43(2):421–9.

[16] Selvakumar PM, Suresh E, Subramanian PS. Single stranded helical supramolecular architecture with a left handed helical water chain in ternary copper(II) tryptophan/diamine complexes. Polyhedron 2009;28(2): 245–52.

[17] Subramanian PS, Suresh E, Casella L. Supramolecular helical architectures dictated by folded and extended conformations of the amino acid in ternary Cu^{II}/diamine/racemic amino acid complexes. Eur J Inorg Chem 2007;2007(12): 1654–60.

[18] Katagiri H, Miyagawa T, Furusho Y, Yashima E. Synthesis and optical resolution of a double helicate consisting of ortho-linked hexaphenol strands bridged by spiroborates. Angew Chem Int Ed 2006;45(11):1741–4.

[19] Albrecht M, Janser I, Kamptmann S, Weis P, Wibbeling B, Fröhlich R. Dicatechol-diimines: easily accessible ligands for the self-assembly of dinuclear triple-stranded helicates. Dalton Trans 2004;2004(1):37–43.

[20] Mateos-Timoneda MA, Crego-Calama M, Reinhoudt DN. Supramolecular chirality of self-assembled systems in solution. Chem Soc Rev 2004;33(6): 363–72.

[21] Piguet C, Bernardinelli G, Hopfgartner G. Helicates as versatile supramolecular complexes. Chem Rev 1997;97(6):2005–62.

[22] Hannon MJ, Childs LJ. Helices and helicates: beautiful supramolecular motifs with emerging applications. Supramolecular Chem 2004;16(1):7–22.

[23] Bünzli J-CG, Piguet C. Taking advantage of luminescent lanthanide ions. Chem Soc Rev 2005;34(12):1048–77.

[24] Albrecht M, Osetska O, Fröhlich R, Bünzli J-CG, Aebischer A, Gumy F, et al. Highly efficient near-IR emitting Yb/Yb and Yb/Al helicates. J Am Chem Soc 2007;129(46):14178–9.

[25] Albrecht M, Fiege M, Kögerler P, Speldrich M, Fröhlich R, Engeser M. Magnetic coupling in enantiomerically pure trinuclear helicate-type complexes formed by hierarchical self-assembly. Chem Eur J 2010;16(29):8797–804.

[26] Matthews CJ, Onions ST, Morata G, Davis LJ, Heath SL, Price DJ. A self-assembled tetracopper triple-stranded helicate: towards the controlled synthesis of finite one-dimensional magnetic chains. Angew Chem Int Ed 2003;42(27):3166–9.

[27] Reichardt C. Solvatochromic dyes as solvent polarity indicators. Chem Rev 1994;94(8):2319–58.

[28] Bamfield P. Chromic phenomena: technological applications of colour chemistry. p. 8. Springer Verlag; 2002.

[29] Narayanan B, Bhadbhade MM. X-Ray structure of thermochromic bis(N, N-Diethylethylenediamine)-copper(II)tetrafluoroborate. J Coord Chem 1998; 46(1):115–23.

[30] Kuroiwa K, Oda N, Kimizuka N. Supramolecular solvatochromism. Effect of solvents on the self-assembly and charge transfer absorption characteristics of lipid-packaged, linear mixed-valence platinum complexes. Sci Technol Adv Mater 2006;7(7):629–34.

[31] El-Ayaan U, Murata F, Fukuda Y. Thermochromism and solvatochromism in solution. Monatschefte Fur Chemie 2001;132(11):1279–94.

[32] Baho N, Zargarian D. Syntheses, structures, spectroscopy, and chromotropism of new complexes arising from the reaction of nickel(II) nitrate with diphenyl(dipyrazolyl)methane. Inorg Chem 2007;46(1):299–308.

[33] Averseng F, Lacroix PG, Malfant I, Lenoble G, Cassoux P, Nakatani K, et al. Synthesis, crystal structure, and second-order nonlinear optical properties of a new bis(salicylaldiminato)nickel(II) metal complex. Chem Mater 1999; 11(4):995–1002.

[34] Ishida M, Naruta Y, Tani F. Copper(II) and nickel(II) hexafluorophosphate complexes derived from a monoanionic porphyrin analogue: solvato- and thermochromism of the Ni complexes by spin-interconversion. Dalton Trans 2010;39(10):2651–9.

[35] Ohtsu H, Tanaka K. Equilibrium of low- and high-spin states of Ni (II) complexes controlled by the donor ability of the bidentate ligands. Inorg Chem 2004;43(9):3024–30.

[36] Chen C-T, Liao S-Y, Lin K-J, Chen C-H, Lin T-YJ. Structural effects on molecular dipoles and solvatochromism of nickel(diimine)(dithiolate) complexes. Inorg Chem 1999;38(11):2734–41.

[37] Miyamae H, Kudo H, Hihara G, Sone K. Solvatochromism and structure of acetylacetonatocopper(II) complexes with *N*,*N*′-dipropyl-, *N*,*N*,*N*′,*N*′-tetrapropyl-, and *N*,*N*- and *N*,*N*′-diisopropylethylenediamines. Bull Chem Soc Jpn 1998;71(11):2621–7.

[38] Meinershagen JL, Bein T. Solvatochromism of a copper(II) (Tetramethylethylenediamine)-(acetylacetonate)$^+$ complex encapsulated in EMT zeolite cages. Adv Mater 2001;13(3):208–11.

[39] Rigamonti L, Demartin F, Forni A, Righetto S, Pasini A. Copper(II) complexes of salen analogues with two differently substituted (Push–Pull) salicylaldehyde moieties. A study on the modulation of electronic asymmetry and nonlinear optical properties. Inorg Chem 2006;45(26):10976–89.

[40] Kurzak K, Kuzniarska-Biernacka I. Spectrochemical properties and solvatochromism of bis(salicylidene-2-amino-3-methylpyridine)copper(II). Struct Chem 2010;21(2):357–66.

[41] Kurzak K, Kuzniarska-Biernacka I, Freire C. Solution properties and solvatochromism of bis(*N*-2-pyridyl-salicylaldiminato)cobalt(II). Struct Chem 2010;21(2):377–83.

[42] Sanders JKM. Adventures in molecular recognition. The ins and outs of templating. Pure Appl Chem 2000;72(12):2265–74.

[43] Hasen Knopf B, Lehn J-M, Kneisel BO, Baum GD, Fenske D. Self-assembly of a circular double helicate. Angew Chem Int Ed 1996;35(16):1838–40.

[44] Schmidtchen FP, Berger M. Artificial organic host molecules for anions. Chem Rev 1997;97(5):1609–46.

[45] Kimura E, Koike T. Dynamic anion recognition by macrocyclic polyamines in neutral pH aqueous solution: development from static anion complexes to an enolate complex. Chem Commun 1998;(15):1495–599. 1998.

[46] Snowden TS, Anslyn EV. Anion recognition: synthetic receptors for anions and their application in sensors. Curr Opin Chem Biol 1999;3(6):740–6.

[47] Albrecht M, Baumert M, Klankermayer J, Kogej M, Shalley CA, Frohlich R. Dicatechol *cis*-dioxomolybdenum(VI): a building block for a lithium cation templated monomer–dimer equilibrium. Dalton Trans 2006;(36):4395–400. 2006.

[48] Goetz S, Kruger PE. A new twist in anion binding: metallo-helicate hosts for anionic guests. Dalton Trans 2006;(10):1277–84. 2006.

[49] Hannon MJ. Supramolecular DNA recognition. Chem Soc Rev 2007;36(2):280–95.
[50] Muller J, Lippert B. Imposing a three-way junction on DNA or recognizing one: a metal triple helicate meets double helix. Angew Chem Int Ed 2006;45(16):2503–5.
[51] Jiang H, Hu A, Lin W. A chiral metallacyclophane for asymmetric catalysis. Chem Commun 2003;(1):96–7. 2003.
[52] Nonius BV. 1998.
[53] Otwinowski Z, Minor W. Processing of X-ray diffraction data collected in oscillation mode. Methods Enzymol 1997;276:307–26.
[54] Otwinowski Z, Borek D, Majewski W, Minor W. Multiparametric scaling of diffraction intensities. Acta Cryst 2003;A59(3):228–34.
[55] Sheldrick GM. Phase annealing in *SHELX*-90: direct methods for larger structures. Acta Cryst 1990;A46(6):467–73.
[56] Sheldrick GM. A short history of *SHELX*. Acta Cryst 2008;A64(1):112–22.
[57] Keller E. SCHAKAL97. Universität Freiburg; 1997.
[58] Keegan J, Kruger PE, Nieuwenhuyzen M, O'Brien J, Martin N. Anion directed assembly of a dinuclear double helicate. Chem Commun 2001;21:2192–3.
[59] Morrison RM, Thompson RC, Trotter J. Evidence for anion coordination in hexafluorophosphate and hexafluoroarsenate complexes of nickel(II). Can J Chem 1980;58(3):238–44.
[60] Constable EC, Hannon MJ, Tocher DA. Dinuclear double helicates incorporating a 1,3-phenylene spacer; the crystal and molecular structure of diacetato-1$x^{2}O$-, 2$x^{2}O$-bis[μ-1,3-bis(4-methylthio-2,2-bipyridin-6-yl)benzene-1$x^{2}N,N$:2$x^{2}N,N$] dinickel bis(hexafluorophosphate). J Chem Soc Dalton Trans 1993;12:1883–90.
[61] Uozumi S, Furutachi H, Ohba M, Okawa H, Fenton DE, Shindo K, et al. Dinuclear nickel(II) complexes of an unsymmetric "End-Off" compartmental ligand: conversion of urea into cyanate at a dinuclear nickel core. Inorg Chem 1998;37(24):6281–7.
[62] Nakamoto K. Infrared spectra of inorganic and coordination compounds. New York: Wiley; 1963. p. 220.
[63] Lewis DL, Estes ED, Hodgson DJ. The infrared spectra of coordinated perchlorates. J Chem Crystallogr 1975;5(1):67–74.
[64] X-ray crystal structure data of 1b: [(C20H22N4)Ni (NCCH3)2]2 4PF6, M = 1498.35, a = 23.9760(2), b = 23.9760(2), c = 40.5393(5)Å, α = 90, β = 90, γ = 120°, V = 20181.8(3)Å3, ρcalc = 1.479 gcm−3, μ = 0.763 mm−1, empirical absorption correction (0.832 ≤ T ≤ 0.862), Z = 12, hexagonal, space group P6/mcc (No.192), λ = 0.71073Å, T = 223(2)K, ω and φ scans, 51538 reflections collected (±h, ±k, ±l), [(sinθ)/λ] = 0.62Å−1, 6658 independent (Rint = 0.063) and 3973 observed reflections [I ≥ 2 σ(I)], 492 refined parameters, R = 0.157, wR2 = 0.392, max. (min.) residual electron density 2.00(-1.35)eÅ−3, hydrogen atoms calculated and refined as riding atoms, anions are heavily disordered, some are only partially occupied, due to this and not localized solvents in voids the analysis is of very limited quality and only done to prove the composition and geometry of the cation.
[65] Linert W, Guttmann V. Structural and electronic responses of coordination compounds to changes in the molecule and molecular environment. Coord Chem Rev 1992;117:159–83.
[66] Sacconi L, Mani F, Bencini A. In: Wilkinson G, Gilard R, Mcleverty J, editors. Nickel in comprehensive coordination chemistry, 5. Pergamon Press: Oxford; 1987. p. 58.
[67] Lever ABP. Inorganic electronic spectroscopy. 2nd ed. Amsterdam, The Netherlands: Elsevier Science; 1984.
[68] M–C Nolet, Beaulac R, Boulanger A-M, Reber C. Allowed and forbidden d-d bands in octahedral coordination compounds: intensity borrowing and interference dips in absorption spectra. Struct Bonding 2004;107:145–58.